# Reevaluation of the Additivity Relationship for Vanadyl−Imidazole Complexes: Correlation of the EPR Hyperfine Constant with Ring Orientation

**Thomas S. Smith, II, Charles A. Root,† Jeff W. Kampf, Paul G. Rasmussen, and Vincent L. Pecoraro***

*Contribution from the Department of Chemistry, The University of Michigan, Ann Arbor, Michigan 48109-1055*

*Received May 10, 1999*

**Abstract:** Five new vanadyl−imidazole complexes with the imidazole ring in different orientations to the vanadyl unit have been synthesized and characterized by X-ray crystallography and electron paramagnetic resonance (EPR). The hyperfine coupling constants ($A_{||}$) from the EPR spectra of these complexes were analyzed using the additivity relationship. There is some discussion as to what contribution an "aromatic imine" such as imidazole bound in the equatorial plane of a vanadyl complex makes to the hyperfine coupling. This analysis, applied to the new complexes as well as those vanadyl−imidazole complexes previously published, reveals a trend in the contribution to the hyperfine coupling related to the orientation of the imidazole ring relative to the vanadyl unit; an imidazole parallel to the vanadium−oxygen double bond was found to have a contribution of $40 \times 10^{-4}$ cm$^{-1}$, while one perpendicular gave a contribution of $45 \times 10^{-4}$ cm$^{-1}$. A similar trend for imine values was also observed in the study of these complexes. These findings will significantly influence EPR studies of vanadium in biological systems, whether naturally occurring or substituted in as a spectroscopic probe. These data are also used to draw structural conclusions on molecules containing vanadyl ion whose structures are not published, including the reduced vanadium bromoperoxidase (VBrPO).

## Introduction

The biological chemistry of vanadium spans native biomolecules as well as systems whose structure or function can be probed or modified by this trace element. Vanadium is found naturally in several marine species,[1] is essential for the function of some nitrogenases[2] and the vanadium haloperoxidases (VHPOs),[3] acts as an insulin mimic,[4] and has been shown to photocleave proteins.[5] The vanadyl ion ($VO^{2+}$) has been used in EPR and ESEEM studies as a probe of spectroscopically silent divalent metal binding sites in a number of biological molecules in which vanadium does not occur naturally, including insulin,[6] carboxypeptidase A,[7] carbonic anhydrase,[8] pyruvate kinase,[9] *S*-adenosyl methionine synthetase,[10] D-xylose isomerase,[11] apoferritin,[12] lactoferrin and transferrin,[13] chloroplast $F_1$-ATPase,[14] calmodulin,[15] collagen,[16] nephrocalcin,[17] and, more recently, imidazole glycerol phosphate dehydratase.[18]

The use of vanadium as a spectroscopic probe in biological systems has become very important. Vanadium(V) has properties that make it an attractive NMR nucleus, and in the vanadium(IV) oxidation level the ion is a very sensitive probe of structure using EPR spectroscopy. Information on the number and types of donors cis to the vanadyl ion can be readily obtained from the EPR hyperfine coupling value $A_{||}$ by application of the additivity relations proposed by Wüthrich and further developed by Chasteen and, later, Cornman.[19,20,21] Unfortunately, axial ligation is not clarified by this approach.

VHPOs have one crystal structure known, that of the vanadium chloroperoxidase (VClPO) from *Curvularia inaequalis*, where one (and only one) protein ligand is bound, an imidazole bound axially[22] (Figure 1). The reduced form of vanadium bromoperoxidase (VBrPO) is catalytically inactive, but can be reoxidized to an active form. Previous studies by

* To whom correspondence should be addressed.
† Permanent Address: The Department of Chemistry, Bucknell University, Lewisburg, PA 17837.

(1) Henze, M. *Hoppe-Seyler's Z. Physiol. Chem.* **1911**, *72*, 494−501.
(2) Eady, R. R. *Vanadium Nitrogenases*; Eady, R. R., Ed.; Kluwer Academic Publishers: Boston, 1990; pp 99−127.
(3) Vilter, H. *Phytochemistry* **1984**, *23*, 1387−1390.
(4) Tolman, E. L.; Barris, E.; Burns, M.; Pansisni, A.; Partridge, R. *Life Sci.* **1979**, *25*, 1159.
(5) Lee-Eiford, A.; Ow, R. A.; Gibbons, I. R. *J. Biol. Chem.* **1986**, *261*, 2337−2342.
(6) Chasteen, N. D.; DeKoch, R. J.; Rogers, B. L.; Hanna, M. W. *J. Am. Chem. Soc.* **1973**, *95*, 1301−1309.
(7) DeKoch, R. J.; West, D. J.; Cannon, J. C.; Chasteen, N. D. *Biochemistry* **1974**, *13*, 4347−4354.
(8) Fitzgerald, J. J.; Chasteen, N. D. *Biochemistry* **1974**, *13*, 4338−4346.
(9) Tipton, P. A.; McCracken, J.; Cornelius, J. B.; Peisach, J. *Biochemistry* **1989**, *28*, 5720.
(10) Zhang, C.; Markham, G. D.; LoBrutto, R. *Biochemistry* **1993**, *32*, 9866−9873.
(11) Dikanov, S. A.; Tyryshkin, A. M.; Hüttermann, J.; Bogumil, R.; Witzel, H. *J. Am. Chem. Soc.* **1995**, *117*, 4976−4986.
(12) Hanna, P. M.; Chasteen, N. D.; Rottman, G. A.; Aisen, P. *Biochemistry* **1991**, *30*, 9210−9216.
(13) Eaton, S. S.; Dubach, J.; More, K. M.; Eaton, G. R.; Thurman, G.; Ambruse, D. B. *J. Biol. Chem.* **1989**, *264*, 4776.
(14) Houseman, A. L. P.; Morgan, L.; LoBrutto, R.; Frasch, W. P. *Biochemistry* **1994**, *33*, 4910.
(15) Nieves, J.; Kim, L.; Puett, D.; Echegoyen, L.; Benabe, J.; Martinez-Maidonado, M. *Biochemistry* **1987**, *26*, 4523−4526.
(16) Ferrari, R. P. *Inorg. Chim. Acta* **1990**, *176*, 83−86.
(17) Mustafi, D.; Nakagawa, Y. *Biochemistry* **1996**, *35*, 14703−14709.
(18) Petersen, J.; Hawkes, T. R.; Lowe, D. J. *J. Am. Chem. Soc.* **1998**, *120*, 10978−10979.
(19) Wüthrich, K. *Helv. Chim. Acta* **1965**, *48*, 1012.
(20) Chasteen, N. D. In *Biological Magnetic Resonance*; Berliner, L. J., Reuben, J., Eds.; Plenum Press: New York, 1981; Vol. 3, pp 53−119.
(21) Cornman, C. R.; Zovinka, E. P.; Boyajian, Y. D.; Geiser-Bush, K. M.; Boyle, P. D.; Singh, P. *Inorg. Chem.* **1995**, *34*, 4213−4219.

10.1021/ja991552o CCC: $19.00 
Published on Web 01/25/2000

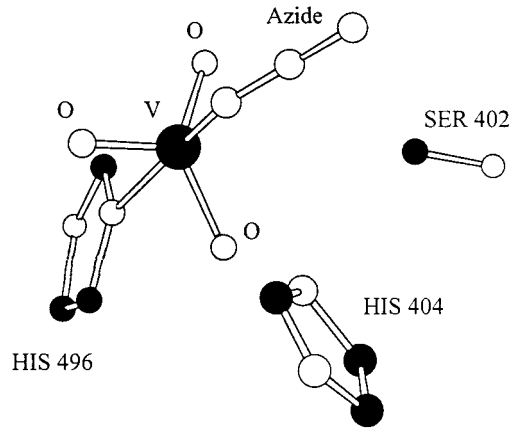


**Figure 1.** Environment of the vanadium atom from the crystal structure of the vanadium chloroperoxidase from *Curvularia inaequalis*, adapted from ref 22a. Carbon and vanadium atoms are black, and nitrogen and oxygen atoms are white.

our group with Frasch and LoBrutto show two different nitrogens bound, which we had tentatively assigned as two imidazoles—one bound axially, the other equatorially.[23] The second imidazole is postulated to be from HIS 404, which is a nearby imidazole perhaps used as an acid/base catalyst in the active enzyme. EPR of the reduced VBrPO gives $A_{||}$ values of $166.6 \times 10^{-4}$ cm$^{-1}$ for the low-pH form and $159.9 \times 10^{-4}$ cm$^{-1}$ for the high-pH form.[24] We have proposed ligand sets for the reduced VBrPO using these numbers. Recent work by Fukui and co-workers agrees with our proposal that there are two imidazoles bound to vanadium in the reduced VBrPO, but proposes that both imidazoles are bound symmetrically in the equatorial plane.[25] In light of our observations herein, we now propose that both imidazoles are in the equatorial plane, but are bound with different orientations with respect to the vanadyl unit. New ligand sets for the reduced VBrPO will be proposed here, using the $A_{||}$ values determined for different orientations of the imidazole ring.

One stumbling block to the general use of the additivity relations in biological systems has been the different reported values for "aromatic imine" donors such as imidazole. There are three common values used for "aromatic imine," only one of which uses an imidazole complex (albeit one with no published crystal structure) as the basis for the number. Cornman et al. report an $A_{||} = 38.3 \times 10^{-4}$ cm$^{-1}$ using $VO(pic)_2$;[21] Chasteen's $A_{||}$ of $40.7 \times 10^{-4}$ cm$^{-1}$ is from $[VO(bipy)_2]^{2+}$;[20] and van Willigen and co-workers have published an $A_{||} = 40.5 \times 10^{-4}$ cm$^{-1}$ from $[VO(im)_4]^{2+}$.[26] In this paper, we will reevaluate the conclusions we have recently presented for the reduced VBrPO. We will also introduce five new crystallographically characterized vanadyl imidazole compounds with different orientations of the imidazole ring with respect to the V=O vector. We will use these model compounds together with previously published compounds to show that the contribution to the $A_{||}$ separation in the EPR spectrum is dependent on the orientation of the rings relative to the vanadyl unit. We shall also present evidence that this orientation effect applies to other imine donors.

## Materials and Methods

The following abbreviations are used throughout the text: HSalimH = 4-(2-(salicylideneamino)ethyl)imidazole; HSalimRH = *N*-(*o*-hydroxyphenyl)histamine; HSalBz = *N*-salicylidene-benzylamine; Hacac = 2,4-pentanedione; $H_2$MDCI = 1-methyl-4,5-dicarboxyimidazole; $H_2$-dipic = 2,6-pyridinedicarboxylic acid.

4,5-Dicyanoimidazole was purchased from TCI America and used as received. Acetonitrile was treated with copper sulfate and distilled from phosphorus pentoxide before use. All other chemicals were purchased from Aldrich Chemical Co. and used as received.

EPR experiments were carried out at X-band (9.33 GHz) using a Bruker 300 EPX spectrometer. DPPH was used as an external reference for *g* values, and the exact spectrometer frequency was monitored with a Hewlett-Packard 5350B microwave frequency counter. $^1$H NMR spectra were obtained on a Bruker 300 MHz instrument updated with a Varian Mercury console. Elemental analyses were performed by the University of Michigan Microanalysis Laboratory. Fast atom bombardment mass spectrometry was performed by the University of Michigan Mass Spectrometry Facility.

**Preparation of Compounds.** Reactions were performed in air, and solvents other than acetonitrile were used as received. Vanadyl sulfate was assumed to be the trihydrate. All ligands synthesized were isolated prior to use. The synthesis of $H_2$MDCI was similar to previous preparations.[27] HSalBz was synthesized by the method of Mason and Winder.[28] $VO(SalBz)_2$ was synthesized by the procedure reported by Cornman and co-workers for the synthesis of bis(*N*-methylsalicylaldiminato)oxovanadium(IV), using HSalBz as the ligand.[29] The presence of vanadium(IV) in $VO(SalBz)_2$ was confirmed by EPR. Anal. Calcd (found) for $C_{28}H_{24}N_2O_3V$ (MW 487.45): C, 68.99 (68.69); H, 4.96 (5.26); N, 5.75 (5.78).

**HSalimRH·2HCl.** Histamine dihydrochloride (8.776 g, 47 mmol) was suspended in 150 mL of methanol. Two equivalents of solid NaOH (3.76 g, 94 mmol) were added slowly, dissolving the histamine and precipitating NaCl. The sodium chloride was filtered off, and salicylaldehyde (5.0 mL, 47 mmol) was added to give a bright yellow solution. The reaction mixture was stirred for an hour. Sodium borohydride (888 mg, 24 mmol) was added slowly over 2 h to the solution, which was then allowed to stir overnight. The resulting pale yellow solution was acidified with concentrated HCl and evaporated to near dryness to give a wet, white residue. This residue was washed with ethanol, then diethyl ether to give the crude product as the HCl salt. If further purification was necessary, the crude product was stirred in a minimal amount of ethanol containing approximately two equivalents of triethylamine and the undissolved sodium chloride filtered off. The filtrate was acidified with concentrated HCl to precipitate the product. Final yield = 9.1 g (67%). $^1$H NMR ($D_2O$): $\delta$ 8.60 (s, 1), 7.36 (m, 3), 6.98 (m, 2), 4.28 (s, 2), 3.40 (t, 2), 3.19 (t, 2). Anal. Calcd (found) for $C_{12}H_{17}N_3OCl_2$ (MW 290.30): C, 49.65 (49.32); H, 5.90 (5.82); N, 14.48 (14.31).

**VO(SalimRH)(acac) (1).** Vanadyl acetoacetonate (1.978 g, 7.46 mmol) and HSalimRH·2HCl (2.164 g, 7.46 mmol) were dissolved in 125 mL methanol to give a dark green solution. Two equivalents of sodium hydroxide in methanol were added rapidly to the solution, which immediately turned wine-red. Stirring was continued for an hour, and a red solid began precipitating from solution. The solution was concentrated, leading to additional red precipitate which was filtered off. The product was washed with water and three times with diethyl ether. Yield = 2.670 g (93%). X-ray quality crystals were obtained after a few days by cooling the reaction mixture to −20 °C immediately after the addition of base. IR (KBr, cm$^{-1}$): 3199.1, 2857.2(b), 2627.1(w), 1605.7(s), 1517.9(s), 1484.2, 1398.3(s), 1270.2(s), 1024.1,

(22) (a)Messerschmidt, A.; Wever, R. *Proc. Natl. Acad. Sci. U.S.A.* **1996**, *93*, 392−396. (b) Messerschmidt, A.; Prade, L.; Wever, R. *Biol. Chem.* **1997**, *378*, 309−315. (c) Macedo-Ribeiro, S.; Hemrika, W.; Renirie, R.; Wever, R.; Messerschmidt, A. *J. Biol. Inorg. Chem.* **1999**, *(4): 2*, 209−219.

(23) LoBrutto, R.; Hamstra, B. J.; Colpas, G. J.; Pecoraro, V. L.; Frasch, W. D. *J. Am. Chem. Soc.* **1998**, *120*, 4410−4416.

(24) de Boer, E.; Boon, K.; Wever, R. *Biochemistry* **1988**, *27*, 1629−1635.

(25) Fukui, K.; Ohya-Nishiguchi, H.; Kamada, H. *Inorg. Chem.* **1998**, *37*, 2326−2327.

(26) Mulks, C. F.; Kirste, B.; van Willigen, H. *J. Am. Chem. Soc.* **1982**, *104*, 5906−5911.

(27) O'Connell, J. F.; Parquette, J.; Yelle, W. E.; Wang, W.; Rapoport, H. *Synthesis* **1988**, *10*, 767−771.

(28) Mason, A. T.; Winder, G. R. *J. Chem. Soc.* **1894**, *65*, 191.

(29) Cornman, C. R.; Geiser-Bush, K. M.; Rowley, S. P.; Boyle, P. D. *Inorg. Chem.* **1997**, *36*, 6401−6408.

**Table 1.** Summary of Crystallographic Data for **1**−**3**

| | VO(SalimRH)(acac) (**1**) | $VO(H_2O)(HMDCI)_2$ (**2**) | $[VO(dipic)(HMDCI)]^-$ (**3**) |
|---|---|---|---|
| formula | $C_{17}H_{21}N_3O_4V$ | $C_{12}H_{15}N_4O_{11.5}V$ | $C_{21}H_{28}N_4O_9V$ |
| *a*, Å | 7.1004(6) | 27.3557(8) | 7.91940(10) |
| *b*, Å | 14.1176(11) | 10.2703(2) | 10.0286(2) |
| *c*, Å | 17.8887(14) | 13.0845(3) | 15.4230(3) |
| α, degrees | 90 | 90 | 96.4410(10) |
| *β*, degrees | 97.5940(10) | 107.6070(10) | 90.5170(10) |
| *γ*, degrees | 90 | 90 | 105.7320(10) |
| crystal system | monoclinic | monoclinic | triclinic |
| space group | $P2_1/c$ | *Cc* | $P\bar{1}$ |
| $d_{calc}$, g/cm$^3$ | 1.429 | 1.707 | 1.508 |
| $d_{obs}$, g/cm$^3$ | 1.403 | 1.674 | 1.481 |
| *Z* | 4 | 8 | 2 |
| cryst appearance | red needles | blue plates | green multifaceted |
| cryst size, mm | 0.22 × 0.04 × 0.04 | 0.16 × 0.16 × 0.36 | 0.16 × 0.16 × 0.16 |
| reflections collected | 8397 | 19344 | 33348 |
| unique data | 3117 | 9471 | 10849 |
| 2*θ* range, degrees | $1 < \theta < 25$ | $2 < \theta < 32$ | $3 < \theta < 36$ |
| largest peak, hole (eA$^{-3}$) | 0.703, −0.284 | 0.418, −0.437 | 0.473, −0.388 |
| R1, wR2 (all data) | 0.0871, 0.1424 | 0.0355, 0.0773 | 0.0912, 0.1046 |
| R1, wR2 ($I > 2\sigma$ data) | 0.0631, 0.1315 | 0.0315, 0.0742 | 0.0531, 0.0909 |

940.5(s), 754.5. Anal. Calcd (found) for $C_{17}H_{21}N_3O_4V$ (MW 382.31): C, 53.41 (53.25); H, 5.54 (5.51); N, 10.99 (11.01). MS (FAB+): *m*/*e* = 383 (M + 1).

**$VO(H_2O)(HMDCI)_2\cdot 1.5H_2O$ (2·1.5$H_2O$).** Barium chloride dihydrate (1.198 g, 4.90 mmol) was added to a solution of vanadyl sulfate hydrate (1.065 g, 4.90 mmol) in 80 mL water. The barium sulfate precipitate was filtered off. $H_2$MDCI (1.669 g, 9.81 mmol) was suspended in 30 mL water. Tetraethylammonium hydroxide (6.96 mL, 9.81 mmol) in water was added to the suspension, dissolving most of the suspended solid. This solution was added to the vanadyl-containing filtrate to give a cloudy, dark blue solution. The reaction was allowed to stir overnight. The resulting blue precipitate was filtered and washed with diethyl ether. This crude product can be recrystallized from hot water. Final yield = 1.363 g (66%). IR (KBr, cm$^{-1}$): 3600.0(b), 3130.6(s), 3000.0(b), 1729.8(s), 1700.1(s), 1615.1(sh), 1577.4(s), 1521.3(s), 1455.4, 1287.2(s), 983.1(s). Anal. Calcd (found) for $C_{12}H_{15}N_4O_{11.5}V$ (MW 450.21): C, 32.01 (32.32); H, 3.36 (3.36); N, 12.44 (12.47). MS (FAB+): *m*/*e* = 406 (M + 1−2.5 $H_2O$).

**$[(CH_3CH_2)_4N][VO(dipic)(HMDCI)]$ (3).** $VO(H_2O)(HMDCI)_2\cdot 1.5H_2O$ (281 mg, 0.65 mmol) was dissolved with heating in 25 mL water. $H_2$dipic (109 mg, 0.65 mmol) was dissolved in 15 mL water by the addition of tetraethylammonium hydroxide (0.46 mL, 0.65 mmol) in water. This ligand solution was added to the blue vanadium complex solution once it had cooled to room temperature. The solution immediately turned green, and was allowed to stir for 2 h. The solvent was removed, leaving behind an oily green residue. The residue was extracted with acetonitrile, and the remaining white solid was filtered off. The green filtrate was allowed to slowly evaporate to give dark green crystals. Yield = 163 mg (47%). IR (KBr, cm$^{-1}$): 3093.0, 3022.6, 2987.5, 1721.9(sh), 1658.6(s), 1574.2, 1525.0, 1328.1, 1173.4, 1082.0, 976.6(s), 913.3, 779.7, 744.5. Anal. Calcd (found) for $C_{21}H_{28}N_4O_9V$ (MW 531.39): C, 47.47 (47.17); H, 5.31 (5.52); N, 10.54 (10.66). MS (FAB−): *m*/*e* = 401 (M(anion)).

**$VO(H_2O)(acac)(HMDCI)$ (4).** $H_2$MDCI (380 mg, 2.23 mmol) was dissolved with heating in 80 mL water. While still warm, this cloudy solution was poured into a solution of vanadyl acetoacetonate (592 mg, 2.23 mmol) in 80 mL methanol. The green solution immediately turned greenish-blue. After the reaction was allowed to cool to room temperature and then stirred for an hour, a small amount of unreacted $H_2$MDCI was filtered off. The filtrate was allowed to slowly evaporate over several days to give purple crystals. Yield = 507 mg (68%). IR (KBr, cm$^{-1}$): 3236.8(vb), 3100.1(s), 1740.9(s), 1569.6(sh), 1531.8(b), 1423.0, 1364.4(s), 1280.4, 1211.6, 968.4(s), 786.4, 766.0. Anal. Calcd (found) for $C_{11}H_{14}N_2O_8V$ (MW 353.18): C, 37.41 (37.48); H, 4.00 (4.01); N, 7.93 (7.92). MS (FAB+): *m*/*e* = 336 (M + 1 − $H_2O$).

**$VO(SalimH)(SalBz)\cdot CH_3OH$ (5·MeOH).** Histamine dihydrochloride (283 mg, 1.54 mmol) was suspended in 50 mL of methanol. Two equivalents of solid NaOH (123 mg, 3.08 mmol) were added, dissolving the histamine. Salicylaldehyde (0.164 mL, 1.54 mmol) was then added to give a bright yellow solution. This mixture was stirred for 15 min. $VO(SalBz)_2$ (750 mg, 1.54 mmol) was added directly to this mixture, and 25 mL ethanol was added to enhance solubility. The reaction was stirred overnight, over which time the green $VO(SalBz)_2$ slowly dissolved and red-orange **5** precipitated out. This was filtered off and washed with ether. X-ray-quality crystals of **5·MeOH** were grown from warm methanol. Yield = 673 mg (89%). IR (KBr, cm$^{-1}$): 3112.2(w,b), 2955.1(w,b), 1617.4(s), 1512.1, 1323.8, 1167.3, 935.1(s), 760.1. Anal. Calcd (found) for $C_{26}H_{24}N_4O_3V\cdot 0.5\ CH_3OH$ (MW 507.46): C, 62.75 (62.52); H, 5.16 (5.14); N, 11.05 (11.41). FAB mass spectroscopy destroyed the complex, yielding only fragment peaks for each ligand in a 1:1 ratio.

**Table 2.** Summary of Crystallographic Data for **4**,**5**

| | $VO(H_2O)(HMDCI)(acac)$ (**4**) | VO(SalimH)(SalBz) (**5**) |
|---|---|---|
| formula | $C_{11}H_{14}N_2O_8V$ | $C_{27}H_{28}N_4O_4V$ |
| *a*, Å | 7.86750(10) | 20.4710(3) |
| *b*, Å | 9.02790(10) | 17.46950(10) |
| *c*, Å | 10.88970(10) | 14.77290(10) |
| α, degrees | 81.8570(10) | 90 |
| *β*, degrees | 85.2040(10) | 109.46(10) |
| *γ*, degrees | 67.0390(10) | 90 |
| cryst syst | triclinic | monoclinic |
| space group | $P\bar{1}$ | $C2/c$ |
| $d_{calc}$, g/cm$^3$ | 1.665 | 1.396 |
| $d_{obs}$, g/cm$^3$ | 1.630 | 1.388 |
| *Z* | 2 | 8 |
| cryst appearance | violet prisms | orange-red plates |
| cryst size, mm | 0.44 × 0.32 × 0.22 | 0.06 × 0.16 × 0.20 |
| reflections collected | 8009 | 44919 |
| unique data | 3448 | 5100 |
| 2*θ* range, degrees | $2 < \theta < 29$ | $1 < \theta < 26$ |
| largest peak, hole (eA$^{-3}$) | 0.509, −0.562 | 0.864, −0.342 |
| R1, wR2 (all data) | 0.0360, 0.0913 | 0.0696, 0.1179 |
| R1, wR2 ($I > 2\sigma$ data) | 0.0336, 0.0900 | 0.0550, 0.1110 |

**Structure Determination.** X-ray crystal structure determinations were performed on a standard Siemens SMART CCD-based X-ray diffractometer equipped with a normal focus Mo-target X-ray tube ($\lambda$ = 0.71073 Å) operated at 2000 W power (50 kV, 40 mA) with intensities measured at 158(2) K (Tables 1 and 2). For all samples, the scan width was 0.3° in $\omega$ and the exposure time was 30 s/frame. The frames were integrated with the Siemens SAINT software package with a narrow-frame algorithm. Analysis of the data showed negligible decay

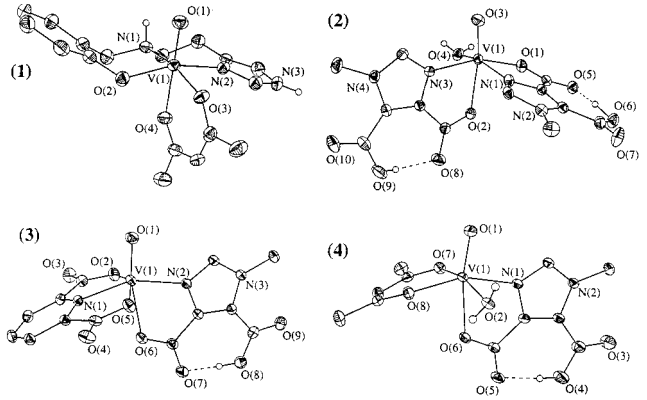


**Figure 2.** ORTEP drawings of complexes **1**−**4**. Thermal ellipsoids are drawn at 50% level of probability. Hydrogens bonded to carbon as well as the tetraethylammonium ion in **3** are not shown for clarity.

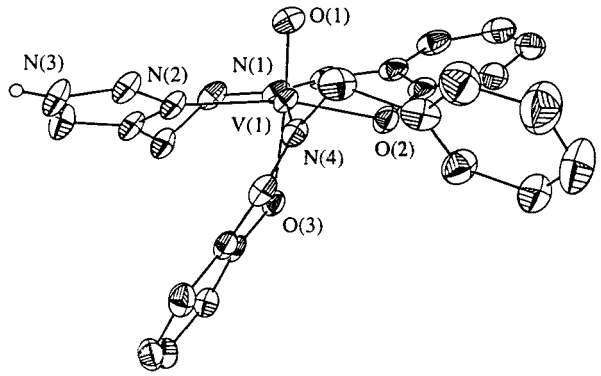

**Figure 3.** ORTEP drawing of complex **5**. Thermal ellipsoids are drawn at 50% level of probability.

during data collection for all samples. The data were corrected for absorption using a multiscan technique (SADABS).[30] The structures were solved and refined with the Siemens SHELXTL (version 5.03) software package.[31] All non-hydrogen atoms were refined anisotropically, with the hydrogen atoms located on a difference Fourier map and allowed to refine isotropically.

**EPR Spectroscopy.** EPR spectra were obtained in frozen solution in dimethylformamide (DMF) at near-liquid nitrogen temperature through the use of a finger Dewar. For those complexes with coordinated water, spectra were also obtained using water/ethylene glycol (1:1) to verify substitution of the bound water by DMF in the DMF solutions. All spectra were simulated with the program Simfonia, bundled with the Bruker EPR software. Reported values of $A_{||}$ are the average result of at least three measurements made on different days with fresh samples. Values of $A_{||}$ are those published by Chasteen,[20] except for the value for coordinated DMF, which was previously reported by this group.[32]

## Results and Discussion

**Description of Structures.** Other than the equatorially bound water in **2** and **4**, the structures of **1**−**5** show few surprises (Figures 2 and 3). The vanadium(IV)−oxo distances fall between 1.591 and 1.622 Å (Table 3). Equatorial V−O distances ranged from 1.962 Å for acac to 2.079 Å for water; all were shorter than the axial V−O bond lengths of 2.155 Å for phenolate, 2.186 Å for acac, and 2.212−2.296 Å for carboxylates. The vanadium−imidazole distances observed were similar to those previously reported,[33,34] with the lengths spanning from

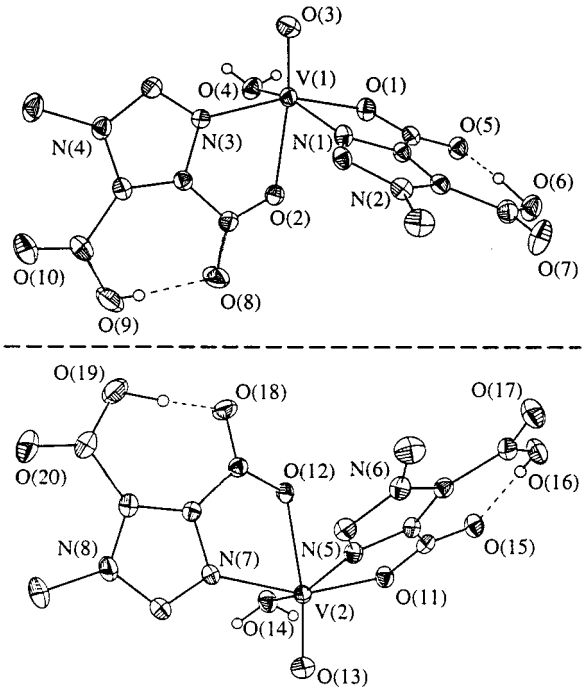

**Figure 4.** ORTEP drawings of the two enantiomers of **2**, emphasizing the mirror plane between them. Both enantiomers are present in each unit cell.

2.075 to 2.121 Å. Vanadium−nitrogen bond distances for parallel and perpendicular orientations of imidazoles and imines are similar. The structure of **1** is predictably similar to that of VO(SalimH)(acac).[33]

The determination of the space group of **2** warrants further discussion. The structure consists of two independent vanadium monomers per asymmetric unit. Initial attempts were made at solving the structure in the centric alternative *C*2/*c* despite the strongly acentric intensity distribution of the data. When no solutions were readily obtained, the acentric alternative was tried and the structure easily solved and refined. Visual inspection of the molecular packing revealed the presence of a near-inversion relationship between the two monomers. One of the monomers was used as a model for a solution in the centric space group via partial structure expansion. A solution was obtained with difficulty in *C*2/*c*; however, the refinement converged at an *R*1 of just under 26%, with a number of unexplained peaks of electron density in chemically unrealistic positions. Further attempts were made to determine a more suitable orientation in the centric lattice via molecular rotations and translations using the program PATSEF, but these models also converged at poor *R* factors. Thus, the acentric space group *Cc* was chosen as the proper description of this structure. The refinement proceeded without any of the typical correlations of geometric oddities associated with a missing inversion center. The calculated Flack parameter indicated the presence of racemic twinning. Introduction of the twinning parameter lowered the residuals from 4.2% to the final converged value of 3.2%. The presence of a racemate is shown from the structure as Figure 4.

**Differences in Contribution to $A_{||}$ by Imidazole Depending on Orientation.** In addition to the new vanadyl imidazole complexes reported here, there are four more published com-

(30) Blessing *Acta Crystallogr.* **1995**, A51, 33−38.
(31) Sheldrick, G. M. *SHELXTL*; Siemens: Madison, WI, 1995.
(32) Hamstra, B. J.; Houseman, A. L. P.; Colpas, G. J.; Kampf, J. W.; LoBrutto, R.; Frasch, W. D.; Pecoraro, V. L. *Inorg. Chem.* **1997**, *36*, 4866−4874.
(33) Cornman, C. R.; Kampf, J.; Lah, M. S.; Pecoraro, V. L. *Inorg. Chem.* **1992**, *31*, 2035−2043.
(34) Calviou, L. J.; Arber, J. M.; Collison, D.; Garner, C. D.; Clegg, W. *J. Chem. Soc., Chem. Commun.* **1992**, 654−656.

**Table 3.** Representative Bond Lengths (in Å) from X-ray Crystallography of **1**−**5**

| | **1** | **2** | **3** | **4** | **5** |
|---|---|---|---|---|---|
| V═O (oxo) | 1.603(3) | 1.591(2) | 1.599(1) | 1.613(1) | 1.622(2) |
| V−O (water) | | 2.020(2) | | 2.079(1) | |
| V−O (acac) | 1.991(3) | | | 1.962(1) | |
| | 2.186(3) | | | 1.985(1) | |
| V−O (equat carboxylate) | | 2.014(2) | 2.014(1) | | |
| | | | 2.027(1) | | |
| V−O (axial carboxylate) | | 2.236(2) | 2.296(1) | 2.212(1) | |
| V−O (equat phenolate) | 1.980(3) | | | | 1.967(2) |
| V−O (axial phenolate) | | | | | 2.115(2) |
| V−N (imidazole) | 2.119(4)[b] | 2.075(2)[b] | 2.087(1)[a] | 2.121(1)[a] | 2.120(2)[b] |
| | | 2.094(2)[a] | | | |
| V−N (pyridine) | | | 2.031(1) | | |
| V−N (imine) | | | | | 2.120(2)[b] |
| | | | | | 2.130(2)[a] |
| V−N (amine) | 2.149(4) | | | | |

[a] Parallel orientation to the vanadyl unit. [b] Perpendicular orientation to the vanadyl unit.

**Table 4.** EPR $g_{\|}$ and $A_{\|}$ Values (in $\times 10^{-4}$ cm$^{-1}$) and Additivity Relationship Contributions

| | $g_{\|}$ | $\|A_{\|}\|$ | $A_{\|}$ contributors other than imidazole[a] | $A_{\|}$ contribution from imidazole(s) | dihedral angle $\theta$ |
|---|---|---|---|---|---|
| VO(SalimRH)(acac) (**1**) | 1.960 | 162.3 | [$R_2NH$] 40.1 | 46.0 | 96.4 |
| | | | [$ArO^-$] 38.6 | | |
| | | | [acac] 37.6 | | |
| VO($H_2O$)(HMDCI)$_2$ (**2**) | 1.955 | 171.0 | [$H_2O$] 45.7 | 83.0 | 6.4 |
| | | | [$RCO_2^-$] 42.7 | (total for both) | 71.7 |
| [VO(dipic)(HMDCI)]$^-$ (**3**) | 1.952 | 167.0 | 2x [$RCO_2^-$] 85.4 | 40.3 | −6.6 |
| | | | [pyridine] 40.7 | | |
| VO($H_2O$)(acac)(HMDCI) (**4**) | 1.960 | 170.0 | eq [acac] 85.0[d] | 39.8 | 1.3 |
| | | | [$H_2O$] 45.7 | | |
| VO(SalimH)(SalBz) (**5**) | 1.962 | 158.9 | 2x [imine] 81.4 | 38.9 | −56.0 |
| | | | [$ArO^-$] 38.6 | | |
| VO(SalimH)(acac)[b] | 1.952 | 162.7 | [imine] 40.7 | 45.8 | 74.9 |
| | | | [$ArO^-$] 38.6 | | |
| | | | [acac] 37.6 | | |
| VO(SalimH)(Sal)[b] | 1.953 | 162.3 | [imine] 40.7 | 44.4 | 68.5 |
| | | | 2x [$ArO^-$] 77.2 | | |
| VO(SalimH)$_2$[b] | 1.953 | 159.6 | 2x [imine] 40.7 | 39.6 | 58.7 |
| | | | [$ArO^-$] 38.6 | | |
| [VO(1-vinylim)$_4$]$^{2+}$ [c] | 1.951 | 162 | | 40.5 | 15.0 (x2) |
| | | | | (each on average) | 25.0 (x2) |

[a] Ref 20. [b] Ref 33. [c] Ref 34. [d] From the EPR of VO(acac)$_2$.

plexes that have been characterized by both X-ray crystallography and EPR.[33,34] By subtracting the contributions of the other coordinated functional groups from the $A_{\|}$ obtained for the complexes, $A_{\|}$ values for imidazole can be obtained. The $A_{\|}$ values for these complexes fell into two groups: one clustered around 40 × 10$^{-4}$ cm$^{-1}$, and one around 45 × 10$^{-4}$ cm$^{-1}$ (Table 4). We also observed that the lower values for $A_{\|}$ tended to be from complexes that contained imidazole rings bound parallel to the vanadyl unit, and the higher values were from complexes where the imidazole was bound perpendicular to the vanadyl unit, or parallel to the equatorial plane of the complex. The dihedral angle $\theta$ is defined by the oxo-vanadium−nitrogen-(2)carbon atoms, and its sign is defined as positive in the counterclockwise direction (Figure 5). A plot of $A_{\|}$ versus the angle of the imidazole ring to the vanadyl unit is shown as Figure 6. Two of the vanadyl−imidazole complexes that have published EPR spectra and crystal structures contain multiple imidazole rings, and for the purpose of plotting that data, the angle of the imidazole rings to the vanadyl unit was considered as a single point at the average of all the angles. This assumption was verified by back-calculation from the obtained curve fit. Error bars were obtained by taking the accepted error in reported complex values (3 × 10$^{-4}$ cm$^{-1}$) and dividing by 4 to get a fixed error of 0.75 × 10$^{-4}$ cm$^{-1}$. Seven of the compounds fall onto a curve defined by $A_{\|} = x + y \sin(2\theta - 90)$, where $x$ and $y$ are the fit parameters. There was no correlation of this difference in $A_{\|}$'s to vanadium−nitrogen bond length or to the distance vanadium is out of the complexes' equatorial plane.

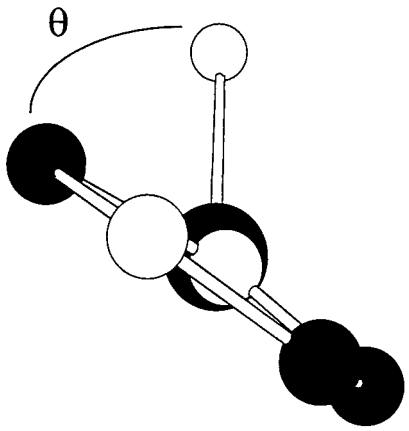


**Figure 5.** Figure illustrating definition of the dihedral angle $\theta$. $\theta$ is defined by the vanadyl oxo, the vanadium atom, the coordinated imidazole nitrogen, and the carbon atom that bridges the two imidazole nitrogens.

The fit to a sine curve is not surprising, given that it is an angle which is being varied. The computed x and $y$ values give a minimum for $A_{\|}$ = 39.76 × 10$^{-4}$ cm$^{-1}$ and a maximum of

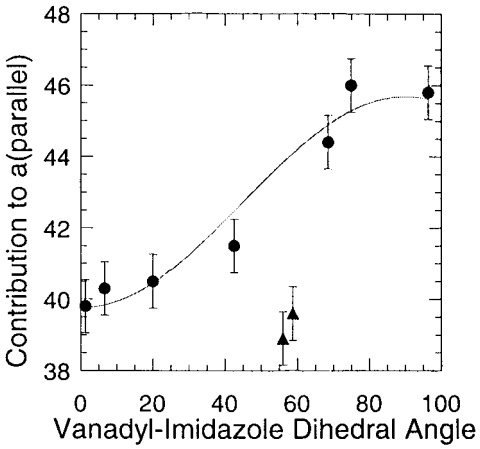


**Figure 6.** Graph plotting the contribution to $A_{||}$ by imidazole (in units of $10^{-4}$ $cm^{-1}$) versus the angle made by the imidazole ring to the vanadyl unit. For simplicity, all angles are shown as being positive. The curve fit is $A_{||} = x + y \sin(2\theta - 90)$ ($x = 42.722$, $y = 2.9638$) and was calculated excluding $VO(SalimH)_2$ and **5**. ($R = 0.977$).

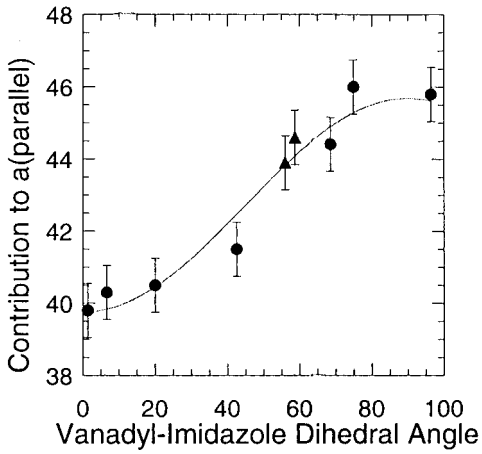


**Figure 7.** Graph plotting the contribution to $A_{||}$ by imidazole versus the angle made by the imidazole ring to the vanadyl unit. In this plot, however, the $A_{||}$ contribution observed from $VO(SalimH)_2$ has been shifted using the assumption that a "perpendicular" imine value would be different by $5 \times 10^{-4}$ $cm^{-1}$ from the typical "parallel" value.

$45.69 \times 10^{-4}$ $cm^{-1}$, or a difference of approximately $6 \times 10^{-4}$ $cm^{-1}$ between the contributions for an exactly parallel imidazole and one at precisely 90° relative to the vanadyl unit.

The outlying complex, $VO(SalimH)_2$, was initially a puzzle. However, it was the only one of the complexes that contained an imine bound in a "parallel" fashion, 90 degrees from the much more prevalent "perpendicular" imine orientation. Thinking it was possible that the difference in $A_{||}$ we observed for imidazole applies to other $sp^2$-hybridized nitrogen donors as well—particularly because Cornman et al. have observed an abnormally low $A_{||}$ for a highly distorted imine complex[29]—we set out to synthesize another vanadyl−imidazole complex containing a parallel bound imine, **5**. As predicted, **5** also did not fit the curve (Figure 6) and gave a calculated $A_{||}$ contribution for imidazole that was low by about the same as that calculated for $VO(SalimH)_2$. Because both $VO(SalimH)_2$ and **5** contain the SalimH ligand bound tridentate in the equatorial plane, verifying the change in the value for the imine was simple and could be done independently of the observed changes for imidazole. By taking the SalimH complex with the vanadyl−imidazole angle closest to these two compounds (VO(SalimH)(Sal)) and subtracting from its $A_{||}$ the known value for phenolate, an $A_{||}$ of $123.7 \times 10^{-4}$ $cm^{-1}$ is obtained for the SalimH ligand as a whole. This value is then subtracted from the $A_{||}$ of $VO(SalimH)_2$ and **5** (159.6 and $158.9 \times 10^{-4}$ $cm^{-1}$, respectively) to give "parallel" imine values of 35.9 and $35.2 \times 10^{-4}$ $cm^{-1}$, respectively. This calculation shows that the magnitude of the change in $A_{||}$ with angle for imines is similar to that for imidazole, approximately $5 \times 10^{-4}$ $cm^{-1}$. When this is taken into account, $VO(SalimH)_2$ and **5** will then fit our observed trend for imidazole orientation (Figure 7).

As always when using characterization in the solid phase (crystallography) to explain observations in solution (EPR), one must remember that the observed solid-state structure may differ from that in solution. We believe this is most likely not the case with these complexes because the DMF/coordinated $H_2O$ substitution is clearly shown (vide infra); the EPR spectra of the five complexes reported here show only one species in solution; and our experience indicates that the complexes do not readily dissociate in solution. Another caveat to researchers studying the EPR and ESEEM of vanadyl complexes is to be careful in assuming that two bidentate ligands will bind exclusively in the equatorial plane. Several recent articles utilizing vanadyl complexes with ligands similar to $H_2$MDCI use this assumption to reach key conclusions.[25,35] In compounds **2** and **4**, we were somewhat surprised to find the solvent molecule bound in the equatorial plane of the complex in the crystal structure. A vanadyl complex with two bidentate ligands not binding exclusively in the equatorial plane has been shown previously by ENDOR studies of the pyridine adduct of VO(acac)$_2$, in which the pyridine binds cis to the vanadyl oxo.[36] The conclusion that the position of the water persists in solution is supported by the observed difference in $A_{||}$ of $2 \times 10^{-4}$ $cm^{-1}$ between samples in water/ethylene glycol and those in DMF. This difference is approximately equal to the difference in contribution to $A_{||}$ between a coordinated water and a coordinated DMF.

**Equatorial vs Axial Ligation Preference of Imidazole to $VO^{2+}$.** One of the original goals of this research was to synthesize a vanadyl complex with an imidazole in the axial position, as there is in the VClPO crystal structure. Our strategy was to block three of the equatorial binding sites with a planar ligand, such as SalimRH or dipic, thereby forcing a second, bidentate ligand to bind at the axial position. This second ligand would then bind through an imidazole nitrogen and another functional group. Because vanadyl complexes prefer oxyanions compared to neutral amines, one might expect that the worst donor ligand (imidazole) would fill the axial position. The other functional group would bind equatorially because it is a better donor than imidazole. The group also should coordinate at a sufficiently low pH to minimize the possibility of oxidation of vanadium(IV) to vanadium(V). $H_2$MDCI was chosen to fulfill all these requirements.

Despite the above reasoning, $H_2$MDCI coordinated to vanadium in all of these cases, with the carboxylate in the axial position. This behavior could be explained by considering the p (aromatic) orbital on the donating nitrogen atom (Figure 8). The imidazole ring will only assume a conformation perpendicular to the vanadyl unit in the equatorial plane when it is constrained by being part of a planar ligand. In the perpendicular conformation, the donating nitrogen p orbital (and, hence, the imidazole's aromatic molecular orbital) can only interact with vanadium d orbitals that are already interacting with the coordination sphere's best $\pi$ donor, the vanadyl oxygen ($d_{xz}$,

(35) Sanna, D.; Micera, G.; Buglyo, P.; Kiss, T.; Gajda, T.; Surdy, P. *Inorg. Chim. Acta* **1998**, *268*, 297−305.

(36) Grant, C. V.; Ball, J. A.; Hamstra, B. J.; Pecoraro, V. L.; Britt, R. D. *J. Phys. Chem. B* **1998**, *102* (42), 8145−8150.

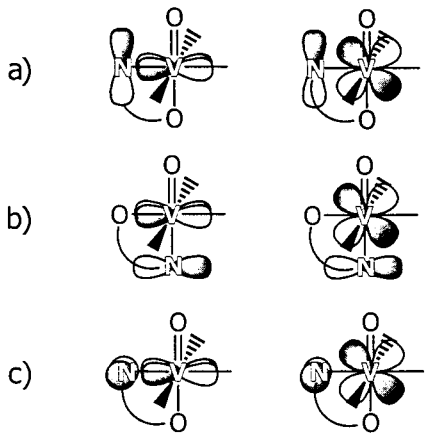


**Figure 8.** Drawings of the overlap of the vanadyl $d_{xy}$, $d_{xz}$, and $d_{yz}$ orbitals with the nitrogen p (aromatic) orbital from the imidazole. (a) The imidazole is bound in the equatorial position and in the perpendicular orientation. (b) The imidazole is bound in the axial position. (c) The imidazole is bound in the equatorial position and in the parallel orientation.

$d_{yz}$). The imidazole ring will prefer not to coordinate in the axial position for the same reason. Only when the imidazole ring coordinates equatorially *and* parallel to the vanadyl unit is the nitrogen's p orbital overlap with the vanadium $d_{xy}$ orbital optimized, and its unfavorable interaction with the $d_{xz}$ and $d_{yz}$ orbitals minimized. We conclude that vanadyl complexes composed of sterically nondemanding ligands which contain coordinated imidazoles will obey this trend for imidazole orientation.

This simple analysis of the orbitals, along with the observed trend in the $A_{||}$ values, led us to consider that the orientation of the ring would also influence the amount of electron donation to the metal by the imidazole. The concept of the imidazole ring's orientation affecting paramagnetic spectroscopy of the metal to which the imidazole is bound is not unheard of. Recently Walker and co-workers have shown the effect of the orientation of an axially bound imidazole on the **g** tensor of iron porphyrins by EPR[37] and ESEEM.[38] Given that, in general, more donating functional groups to vanadium(IV) have a lower contribution to $A_{||}$,[20] ring orientation could be the solution to the problem of the conflicting values for imidazole. An imidazole oriented parallel to the vanadyl unit for best orbital overlap would be a better $\pi$ donor, and so would have a lower contribution to $A_{||}$. This combined with the observed $A_{||}$ values would support the conclusion that van Willigen's value of 40.5 $\times$ $10^{-4}$ $cm^{-1}$ for $[VO(im)_4]^{2+}$ means all four imidazoles are bound parallel to the vanadyl unit. This preference for equatorial binding with parallel orientation also holds true for $[VO(1\text{-vinylimidazole})_4]^{2+}$.[34]

There are two vanadyl−benzimidazole complexes, synthesized by Crans and co-workers, which we have so far left out of consideration.[39] Since benzimidazole may be electronically different enough from imidazole to make comparisons with imidazole complexes invalid, we shall treat them separately here. (*N*-(Benzimidazol-2-ylmethyl)iminodiacetato)-aquo-oxovanadium-(IV) contains a parallel bound benzimidazole with a calculated $A_{||}$ of 39.9 $\times$ $10^{-4}$ $cm^{-1}$, which is in agreement with our observations. For (*N*-(Benzimidazol-2-ylmethyl)imino(ethanol)-ethanolato)-(acetylacetonato)-oxovanadium(IV), Crans notes an unusually high $A_{||}$ and cites the complex's distorted structure as a possible cause. Because this complex contains a coordinated alkoxide group, and because the EPR is performed in a DMF/water solution, it could be possible that the alkoxide has been protonated and/or exchanged for a solvent molecule, which would provide one explanation for the unusually high $A_{||}$. Using the value for an acac bound at two equatorial sites from $VO(acac)_2$, the calculated $A_{||}$ for the benzimidazole ligand in this complex is 45.9 $\times$ $10^{-4}$ $cm^{-1}$, leading us to interpret that the benzimidazole is bound in a perpendicular orientation. Although the crystal structure of this compound shows the benzimidazole bound in a parallel fashion, this could be an indication of ligand reorientation in solution, providing a second possible solution for the complex's unusually high $A_{||}$.

**Table 5.** Complete EPR *g* and A Values (in $\times 10^{-4}$ $cm^{-1}$) and Metal Character of Bonding ($\beta^2$)

| | $g_{||}$ | $A_{||}$ | $g_{\perp}$ | $A_{\perp}$ | $\beta^2$ |
|---|---|---|---|---|---|
| VO(SalimRH)(acac) (**1**) | 1.960 | −162.3 | 1.991 | −57.1 | 0.860 |
| $VO(H_2O)(HMDCI)_2$ (**2**) | 1.955 | −171.0 | 1.994 | −62.1 | 0.907 |
| $[VO(dipic)(HMDCI)]^-$ (**3**) | 1.952 | −167.0 | 1.985 | −59.8 | 0.880 |
| $VO(H_2O)(acac)(HMDCI)$ (**4**) | 1.960 | −170.0 | 1.994 | −61.2 | 0.905 |
| VO(SalimH)(SalBz) (**5**) | 1.962 | −158.9 | 1.990 | −56.1 | 0.844 |
| VO(SalimH)(acac)[a] | 1.952 | −162.7 | 1.977 | −56.7 | 0.852 |
| VO(SalimH)(Sal)[a] | 1.953 | −162.3 | 1.979 | −56.5 | 0.853 |
| $VO(SalimH)_2$[a] | 1.953 | −159.6 | 1.979 | −55.2 | 0.838 |
| $[VO(1\text{-vinylim})_4]^{2+}$ [b] | 1.951 | −162 | 1.983 | −63 | 0.85 |

[a] Ref 33. [b] Ref 34.

**Discussion of Orientation Dependence.** If the change to imidazole's contribution to $A_{||}$ can be considered as resulting from the change in donation from the nitrogen p aromatic orbital into the nonbonding orbital on vanadium containing the unpaired electron, then this effect should also show up as a change in the metal's bonding character. The relationship between the hyperfine coupling constant and bond covalency has been studied by McGarvey,[40] and this concept has been used in a number of systems including Penfield et al.'s studies of the blue copper site.[41] An equation relating the hyperfine coupling constant and *g* values to $\beta^2$, the measure of metal character in bonding, can be derived from the Fermi contact, dipolar coupling, and induced dipolar coupling contributions to $A_{||}$. For vanadyl complexes, that equation is

$$A_{||} = P_d\{[-\kappa - (4/7)]\beta^2 + (g_{||} - 2.0023) + (3/7)(g_{\perp} - 2.0023)\}$$

where $P_d$ = 128 $\times$ $10^{-4}$ $cm^{-1}$ and $\kappa$ = 0.85.[42] Values of $\beta^2$ and complete EPR parameters for all nine vanadyl−imidazole complexes discussed earlier are shown in Table 5. Since the *g* values for all these complexes vary little and are close to 2, the overwhelmingly dominant term is $A_{||}$. Therefore, as the total $A_{||}$ for the complex increases, the metal character of the complexes' metal-to-ligand bonding increases, signifying a reduction in electron donation from the ligands. This can be applied to the specific case of imidazole ligands. An imidazole ring perpendicular to the vanadyl unit has a higher contribution to $A_{||}$, thereby increasing $\beta^2$, which is a sign of lower electron donation by the ligand. A parallel imidazole ring, which has a lower contribution to $A_{||}$, therefore has higher electron donation to the metal. This enhancement of donor ability can be explained by the changing overlap with orientation of the imidazole

(37) Shokhirev, N. V.; Walker, F. A. *J. Am. Chem. Soc.* **1998**, *120*, 981−990.

(38) Raitsimring, A. M.; Walker, F. A. *J. Am. Chem. Soc.* **1998**, *120*, 991−1002.

(39) Crans, D. C.; Keramidas, A. D.; Amin, S. S.; Anderson, O. P.; Miller, S. M. *J. Chem. Soc., Dalton Trans.* **1997**, 2799−2812.

(40) McGarvey, B. R. *J. Phys. Chem.* **1967**, *71*, 1(1), 51−67.

(41) Penfield, K. W.; Gewirth, A. A.; Solomon, E. I. *J. Am. Chem. Soc.* **1985**, *107*, 4519−4529.

(42) Solomon, E. I. Private communication.

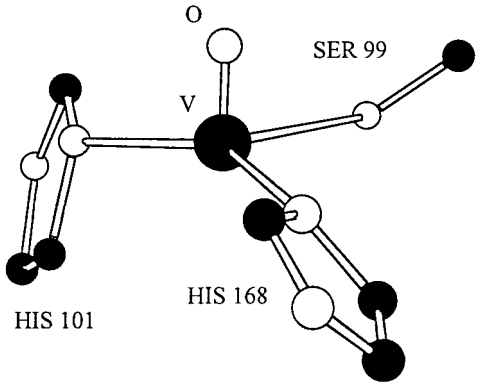


**Figure 9.** Picture of hypothetical ligands to vanadium in the reduced vanadium bromoperoxidase. Carbon and vanadium atoms are black; nitrogen and oxygen atoms are white. The protein ligand positions are taken as those in the VClPO crystal structure in ref 22a, save for the serine side chain which has been rotated to face toward the vanadium. Then the vanadium atom was moved so all metal−ligand distances are less than 3.5 Å. The protein residue numbers given are those for the vanadium bromoperoxidase.

nitrogen p orbital with the vanadium $d_{xy}$ orbital. If one considers the change in the overlap integral between the $d_{xy}$ vanadium orbital and the nitrogen p orbital, the expression for the portion of the integral that depends on $\phi$ is $\int \sin 2\phi \, d\phi$. (Constants, including sign, have been ignored to look at this angular dependence; $\phi$ is the out-of-*xy*-plane angle and corresponds to $\theta$ used for ring orientation.) This evaluates to $-\cos 2\phi$, or $\sin(2\phi - 90)$, which is the dependence on angle we have observed. Therefore, if the overlap between the vanadium $d_{xy}$ and imidazole nitrogen p orbitals increases, there is a larger donation from the aromatic system into the nonbonding orbital, which decreases the metal character of the bonding to the ligand (shown by the change in $\beta^2$). This also decreases the amount the unpaired electron in the nonbonding orbital interacts with the vanadium nucleus, due to the participation of its orbital in bonding with the imidazole aromatic system (shown by the change in $A_{||}$).

**Possible Vanadium Environment in the Reduced VBrPO.** With these proposed $A_{||}$ values for imidazole, an alternate set of ligands to that we had previously proposed[23] can be deduced from the EPR of reduced VBrPO, although the previous ligand sets are still viable. There are two published $A_{||}$ values for reduced VBrPO—one at low pH ($A_{||} = 166.6 \times 10^{-4}$ cm$^{-1}$), the other at high pH ($a_{||} = 159.9 \times 10^{-4}$ cm$^{-1}$).[24] The ligand set [⊥ imidazole, || imidazole, alkoxide, hydroxide] gives a calculated $A_{||} = 160.0 \times 10^{-4}$ cm$^{-1}$, well within the accepted $3 \times 10^{-4}$ cm$^{-1}$ allowable error.[20] For low pH, the ligand set [⊥ imidazole, || imidazole, alkoxide, water] has a calculated $A_{||} = 167.0 \times 10^{-4}$ cm$^{-1}$, which is also in very close agreement to the observed data.

For these proposed sets to have any meaning in reality, the ligands listed should be near the vanadium in the published crystal structure for VClPO, and should be conserved between the sequences of the VClPO and VBrPO being examined. There are two histidines (HIS 404 and HIS 496 in VClPO, HIS 101 and HIS 168 in VBrPO) and a serine (SER 402 in VClPO, SER 99 in VBrPO), all within 5.5 Å of each other and of the vanadium atom.[22] All three of these residues could be brought within 5.5 Å of the vanadium by shifting the metal slightly and rotating the C−C bond in the serine side chain to bring the alcohol closer (Figure 9). Also, the two histidine imidazoles are oriented perpendicular to each other, and the high pH set balances the charge of the vanadyl ion. The placement of both imidazoles in the equatorial plane implies a shifting of the short vanadium−oxygen distance upon reduction of VBrPO, to make the axial imidazole in the original enzyme equatorial. This could explain the difficulty in oxidizing the vanadium back to vanadium(V) to reclaim enzymatic activity.

**Application to Other Systems.** Another example of the application of these new values for imidazole that consider orientation is bovine carboxypeptidase A. When Chasteen and co-workers substituted vanadyl ion for the active site zinc in carboxypeptidase A, an $A_{||}$ of $166.6 \times 10^{-4}$ cm$^{-1}$ at pH > 5 and $175.8 \times 10^{-4}$ cm$^{-1}$ resulted, becoming more dominant below pH 5.[7] The high pH form was assigned to a coordination environment of two imidazoles and two waters, and the low pH form, without a higher value known for imidazoles with a different orientation, was assigned to carboxylate coordination. However, the new values for imidazole can be used to propose a coordination environment of [⊥ imidazole, || imidazole, carboxylate, water] with a calculated $A_{||}$ of $174.4 \times 10^{-4}$ cm$^{-1}$. A ligand set for the higher pH form can be reached by simply deprotonating the water to give [⊥ imidazole, || imidazole, carboxylate, hydroxide] with a calculated $A_{||}$ of $167.4 \times 10^{-4}$ cm$^{-1}$. Lipscomb and co-workers have since solved the X-ray structure of bovine carboxypeptidase A, and their work shows that ligands to the active site zinc are indeed water, carboxylate, and two imidazoles whose ring planes are at right angles to each other.[43]

In light of this trend relating the orientation of the imidazole ring relative to the vanadyl unit to the imidazole's contribution to the observed $A_{||}$ for the complex, the possibility that it could affect other spectroscopic results should be investigated. We recently proposed that a resonance at 4.5 MHz in the ESEEM spectrum of VBrPO could be representative of an axially coordinated nitrogen, most likely an imidazole.[23] An alternative to this proposal would be that, instead of the ESEEM spectrum showing two ligands differing in their sites of coordination to vanadium, the different resonances could be the result of two equatorially coordinated imidazoles with differing orientations relative to the vanadyl unit. The ESEEM spectra of these new model complexes will be investigated in future studies to evaluate this hypothesis.

## Conclusion

We have synthesized and characterized five new vanadyl imidazole complexes, including a complex, **2**, with two imidazoles bound equatorially, but in different orientations relative to the vanadyl unit. These complexes plus the four complexes published previously that have been characterized by EPR and X-ray crystallography show a trend in the observed $A_{||}$ based on the imidazole ring's angle to the vanadyl unit. Imidazoles bound parallel to the vanadyl unit have a contribution to $A_{||}$ of approximately $40 \times 10^{-4}$ cm$^{-1}$, while the contribution for perpendicular imidazoles is close to $45 \times 10^{-4}$ cm$^{-1}$. This trend could be explained by considering the overlap of the imidazole nitrogen p orbital with the vanadium nonbonding $d_{xy}$ orbital (favorable) and with the vanadium $d_{xz}$ and $d_{yz}$ orbitals (unfavorable), a conclusion supported by examination of metal bonding character. This explanation leads to the conclusion that for vanadyl complexes without sterically demanding ligands, imidazole bound equatorially will prefer to be parallel to the vanadyl unit. Imine ligands also appear to have a similar relationship, of similar magnitude, between angle to the vanadyl and contribution to $A_{||}$. This orientation trend may also explain

(43) Rees, D. C.; Lewis, M.; Lipscomb, W. N. *J. Mol. Biol.* **1983**, *168*, 367−387.

our previous observation of two sets of imidazole peaks in the ESEEM spectrum of the reduced VBrPO. The separate values for parallel and perpendicular imidazoles can be used to interpret the published $A_{||}$ values for the reduced VBrPO to give the types of ligands bonded to the vanadium. We propose the ligand set [⊥ imidazole, || imidazole, alkoxide, hydroxide] at high pH and the ligand set [⊥ imidazole, || imidazole, alkoxide, water] at low pH. These sets are possible based on the known residues near the active site in VBrPO.

**Acknowledgment.** This work is supported by a generous grant from the NIH, grant no.: 42703-09. T.S.S. would like to thank Dr. Charles R. Cornman for discussions on EPR simulations, Prof. Edward I. Solomon for discussions on the relationship of the hyperfine coupling constant to bond covalency, and also Dr. Jason Halfen and Mr. Jeffrey Bodwin for their work on the crystal structure of **1**.

**Supporting Information Available:** Complete tables of structure factors and complete atom numbering schemes for **1**−**5** are available as Supporting Information, as well as a representative EPR spectrum of **4** with simulation and a graph of $\beta^2$ versus $A_{||}$ (PDF). An X-ray crystallographic file in CIF format. This material is available free of charge via the Internet at http://pubs.acs.org.

JA991552O